

## Study on the Microstructural Characteristics of an Oxide Layer formed on Zirconium

Hyun-Gil Kim<sup>a,\*</sup>, Byoung-Kwon Choi<sup>a</sup>, Nam-Chan Cho<sup>b</sup>, Chan-Hyun Park<sup>b</sup>, Sun-Doo Kim<sup>b</sup>, Yong-Hwan Jeong<sup>a</sup>

<sup>a</sup>Advanced Core Materials Lab, Korea Atomic Energy Research Institute, Daejeon 305-353, South Korea

<sup>b</sup>Korea Nuclear Fuel Co., Ltd. Daejeon 305-353, South Korea

\*hgkim@kaeri.re.kr

### 1. Introduction

It has been known for a long time that the Zr-based alloys used as fuel cladding in a nuclear reactor have a good corrosion resistance and mechanical properties at a high temperature, and a neutron stability. Corrosion behavior of a zirconium alloy is controlled by its oxide properties such as its grain morphology and crystal structure [1]. It is well known that the formation of a zirconium oxide layer is caused by an oxygen ion diffusion into a zirconium matrix at a high temperature. Generally these oxide characteristics are divided into two significant classifications such as the crystal structure of the tetragonal and monoclinic phases and the grain shapes of the columnar and equiaxed grains. According to previous investigations, the formation of a columnar grain shape and a tetragonal phase in the oxide layer was the main reason for the good corrosion resistance of Zr-based alloys [2]. However, some researchers found that the volume fraction of a tetragonal phase in an oxide layer was not correlated with the corrosion resistance [3]. In this study, the Focused Ion Beam (FIB) milling technique was used for preparing a cross-sectional oxide TEM sample and a High Voltage Electron Microscopy (HVEM) of 1250 keV at the Korea Basic Science Institute (KBSI) was applied to analyze the microstructural characteristics of a zirconium oxide layer. Two types of oxide samples formed on pure-Zr and Zr-1.5Nb alloy were selected for the oxide microstructure observation, because very different corrosion rates were observed in the both alloys. Therefore, the oxide characteristics are compared in terms of their crystal structures (tetragonal and monoclinic grains) and grain morphologies (equiaxed and columnar) in a comparison with their corrosion behavior.

### 2. Experimental procedure

The samples for the corrosion test and oxide analysis of zirconium materials were selected from pure-Zr and Zr-1.5 wt.%Nb alloy. Both materials were prepared by a vacuum arc re-melting with Zr sponge and high purity (99.99%) Nb and then this ingot was beta-solution treated at 1050 °C for 20 min. The quenched ingot was hot-rolled after a pre-heating at 580 °C for 10 min and cold-rolled three times to a final thickness of 1 mm. Between the rolling steps, the cold rolled sheet was intermediate-annealed at 580 °C to control the type of the second phase

as a  $\beta$ -Nb phase [4]. Specimens for the corrosion test, 25 x 15 x 1 mm in size, were cut from the sheets, mechanically ground up to 1200 grit SiC paper, and then pickled in a solution of 5 vol.% HF, 45 vol. % HNO<sub>3</sub> and 50 vol.% H<sub>2</sub>O. The corrosion test was performed in a static autoclave with distilled water under the conditions of 360 °C and 18.9 MPa according to the procedure of ASTM G2-88.

To obtain the pre-transition oxides which had nearly equal weight gains, the samples for the oxide characterization were obtained from the pure-Zr and Zr-1.5Nb alloy corroded for 30 and 150 days respectively. For the TEM observation, the corroded samples were prepared by using the FIB milling technique. A HVEM of 1250 keV, where the point resolution of this microscopy is 0.117 nm, was used for the oxide layer analysis. The HVEM had a good point resolution and also a large penetration depth for the samples more so than the conventional TEM.

### 3. Results and discussion

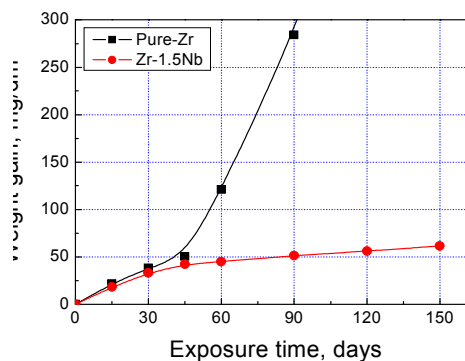


Fig. 1 Corrosion behavior of pure-Zr and Zr-1.5Nb alloy corroded in a static autoclave at 360 °C in a pure water condition

Fig. 1 shows the corrosion behavior of the pure-Zr and Zr-1.5Nb alloy tested in a static autoclave with a 360 °C water condition for up to 150 days. The exposure time steps for measuring the weight gain of both material specimens were 15 and 30 days at periodic terms. A transition behavior was observed in the pure-Zr and the weight gain range at the transition point was about 50-60 mg/dm<sup>2</sup>. The corrosion weight gain of the pure-Zr was considerably increased after a transition. However, a

transition behavior was not observed, but the weight gain was somewhat increased in the Zr-1.5Nb alloy up to a corrosion exposure time of 150 days. So, the corrosion resistance of the Zr-1.5Nb alloy was better than the pure-Zr in the corrosion condition of a 360 °C water.

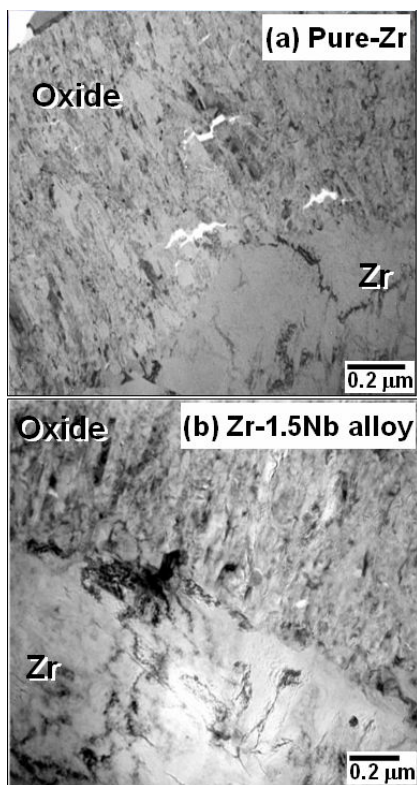


Fig. 2 Cross-sectional oxide morphologies of the oxides of the pure-Zr (a) and Zr-1.5Nb alloy (b)

Fig. 2 shows the cross-sectional oxide morphology of the oxides which were corroded for different times because the corrosion rate was different in both materials. The weight gain of both materials is about 20 mg/dm<sup>2</sup>, which was controlled by the corrosion exposure time, and it could be converted to a corrosion weight gain as follows; 1 μm ≈ 15 mg/dm<sup>2</sup> [5]. So, the oxide thickness of both materials was about 1.3 μm when the cross-sectional observation was matched with the weight gain results. From the view point of an oxide morphology, the outer region of the oxide layer mainly consisted of equiaxed grains of about 0.5 μm in thickness for both materials. Also, the inner region of that layer mainly consisted of columnar grains for the metal/oxide interface area of both materials. From this result, the characteristics of the grain morphology in the oxide layer in the pre-transition region of both materials were very similar.

In general, none-protective oxides are significantly more cracked than protective oxides, and their

oxide/metal interface is more irregular. These cracks and a more irregular oxide/metal interface were observed in the oxide layer formed on the pure-Zr substrate as shown in Fig. 2 (a), whereas, these cracks and an irregular oxide/metal interface were not observed in the oxide layer formed in the Zr-1.5Nb alloy as shown in Fig. 2 (b). The size of the cracks reached 0.2 μm and the width of the irregular oxide/metal interface was about 0.3 μm in the pure-Zr oxide layer. So, the protectiveness of the oxide against a corrosion was decreased in the pure-Zr oxide, although the oxide thickness formed on both pure-Zr and Zr-1.5Nb had a similar thickness of about 1.3 μm. Therefore, it was assumed that the protectiveness of the oxide layer could be affected by the Nb addition as an alloying element.

#### 4. Conclusion

The corrosion behavior and the oxide microstructural characteristics of pure-Zr and Zr-1.5Nb alloy were investigated. The crystalline structure and morphology of a zirconium oxide formed in a water at 360 °C and 18.9 MPa was analyzed by using a Transmission Electron Microscopy (TEM). The corrosion rate was increased more in the pure-Zr than the Zr-1.5Nb alloy after a transition of the corrosion rate. Therefore, it was suggested that the Nb affected the oxide characteristics of the crystal structure and changed the corrosion behaviors.

#### ACKNOWLEDGMENTS

This study was supported by Korean government, through its national nuclear technology program.

#### REFERENCES

- [1] B. Cox, *Advanced in Corrosion Science and Technology*, vol. V, Plenum Press, New York: 173, 1976.
- [2] F. Garzarolli, H. Seidel, R. Tricot, and J.P. Gross, *Zirconium in the Nuclear Industry*, ASTM STP 1132 p. 395, 1991.
- [3] A. Yilmazbayhan, A.T. Motta, R.J. Comstock, G.P. Sabol, B. Lai, Z. Cai, *J. Nucl. Mater.*, 324 p. 6, 2004
- [4] H.G. Kim, J.Y. Park and Y.H. Jeong, *J. Nucl. Mater.*, 347 p. 140, 2005
- [5] J. Krýsa, J. Maivner, P. Matějka and V. Vrtílková, *Mat. Chem. and Phys.*, 63 p.1, 2000